Cambridge Monographs on Mechanics

Theory of Solidification

STEPHEN H. DAVIS

CAMBRIDGE

more information - www.cambridge.org/0521650801

This page intentionally left blank

Theory of Solidification

The processes of freezing and melting were present at the beginnings of the Earth and continue to affect the natural and industrial worlds. The solidification of a liquid or the melting of a solid involves a complex interplay of many physical effects. This book systematically presents the field of continuum solidification theory based on instability phenomena. An understanding of the physics is developed by using examples of increasing complexity with the object of creating a deep physical insight applicable to more complex problems.

Applied mathematicians, engineers, physicists and materials scientists will all find this volume of interest.

Stephen H. Davis is McCormick Professor and Walter P. Murphy Professor of Applied Mathematics at Northwestern University.

CAMBRIDGE MONOGRAPHS ON MECHANICS

FOUNDING EDITOR

G. K. Batchelor

GENERAL EDITORS

THEORY OF SOLIDIFICATION

STEPHEN H. DAVIS
Northwestern University

CAMBRIDGE
UNIVERSITY PRESS

PUBLISHED BY THE PRESS SYNDICATE OF THE UNIVERSITY OF CAMBRIDGE
The Pitt Building, Trumpington Street, Cambridge, United Kingdom

CAMBRIDGE UNIVERSITY PRESS
The Edinburgh Building, Cambridge CB2 2RU, UK
40 West 20th Street, New York, NY 10011-4211, USA
477 Williamstown Road, Port Melbourne, VIC 3207, Australia
Ruiz de Alarcón 13, 28014 Madrid, Spain
Dock House, The Waterfront, Cape Town 8001, South Africa

http://www.cambridge.org

First published in printed format 2001

ISBN 0-511-03696-5 eBook (Adobe Reader)
ISBN 0-521-65080-1 hardback

I dedicate this book to the wonderful women in my life,
my mother Eva
and
my wife Suellen

Contents

Preface

Materials Science is an extremely broad field covering metals, semiconductors, ceramics, and polymers, just to mention a few. Its study is dominated by the *fabrication* of specimens and the *characterization* of their properties. A relatively small portion of the field is devoted to *phase transformation*, the dynamic process by which in the present context a liquid is frozen or a solid is melted.

This book is devoted to the study of liquid (melt)-solid transformations of atomically rough materials: metals or semiconductors, including model organics like plastic crystals. The emphasis is on the use of instability behavior as a means of understanding those processes that ultimately determine the microstructure of a crystalline solid. The fundamental building block of this study is the Mullins–Sekerka instability of a front, which gives conditions for the growth of infinitesimal disturbances of a soild–liquid front. This is generalized in many ways: into the nonlinear regime, including thermodynamic disequilibrium, anisotropic material properties, and effects of convection in the liquid. Cellular, eutectic, and dendritic behaviors are discussed. The emphasis is on dynamic phenomena rather than equilibria. In a sense then, it concerns "physiology" rather than "anatomy."

The aim of this book is to present in a systematic way the field of continuum solidification theory. This begins with the primitive field equations for diffusion and the derivation of appropriate jump conditions on the interface between the solid and liquid. It then uses such models to explore morphological instabilities in the linearized range and gives physical explanations for the phenomena uncovered. To this point the discussion is elementary in terms of mathematical sophistication. It then enters into the nonlinear theories of morphological change with the use of bifurcation theory for wave number and pattern selection, long-wave theories in the strongly nonlinear range, and numerical simulation. The reader is assumed to be reasonably sophisticated in the mathematical methods,

that is, stability theory and its nonlinear extensions and some asymptotic and perturbation theory, but having little background in materials science. Thus, the book is deliberately nonuniform in its "degree of difficulty." Those with limited mathematical background can skip the nonlinear theories and read about the physical phenomena and the linearized theories in the various chapters. The text should take the reader from the elements of the physics to the latest developments of the theory. It would be hoped that applied mathematicians, engineers, and physicists would profit from the material presented as would theoretically inclined materials scientists who could see how mathematics can generate understanding of relevant physical phenomena. An understanding of the physics is developed by using examples of increasing complexity with the objective of creating a deep physical insight applicable to more complex problems.

My interest in solidification was first stimulated by Jon Dantzig in his Ph.D. thesis of 1977 and permanently triggered by Ulrich Müller in our 1984 work on Bénard convection coupled to a freezing front. When learning a new subject as an "adult," one leans heavily on the expertise of senior colleagues for their wisdom. I thus wish to publicly thank Sam Coriell, Jon Dantzig, Paul Fife, Marty Glicksman, Wilfried Kurz, Jeff McFadden, Uli Müller, Bob Sekerka, Peter Voorhees, and Grae Worster for their contributions to my education.

I have always learned more from my graduate students, post-doctoral fellows, and visiting scientists than they have from me. I wish to thank them for their willingness to try something new. They are V. S. Ajaev, K. Brattkus, R. J. Braun, L. Bühler, D. J. Canright, Y.-J. Chen, J. A. Dantzig, A. A. Golovin, H.-P. Grimm, D. A. Huntley, P.-Q. Luo, G. B. McFadden, G. J. Merchant, P. Metzener, U. Müller, D. S. Riley, T. P. Schulze, B. J. Spencer, A. Umantsev, G. W. Young, and J.-J. Xu.

I am grateful to several people for reading selected chapters of the book and making important suggestions. They are Dan Anderson, Kirk Brattkus, Yi-Ju Chen, Jon Dantzig, Sasha Golovin, Jeff McFadden, Tim Schulze, Peter Voorhees, Grae Worster, and J.-J. Xu.

This book could not have been written without the generous support of the National Aeronautics and Space Administration Microgravity Sciences and Applications Program.

Finally, I would like to thank my secretary, Judy Piehl, not only for her impeccable typing, but for her sense of joy in her work. Her presence in the department makes it possible for all of us to do better what we do.

1

Introduction

The processes of freezing and melting were present at the beginning of the Earth and continue to affect the natural and industrial worlds. These processes created the Earth's crust and affect the dynamics of magmas and ice floes, which in turn affect the circulation of the oceans and the patterns of climate and weather. A huge majority of commercial solid materials were "born" as liquids and frozen into useful configurations. The systems in which solidification is important range in scale from nanometers to kilometers and couple with a vast spectrum of other physics.

The solidification of a liquid or the melting of a solid involves a complex-interplay of many physical effects. The solid–liquid interface is an active free boundary from which latent heat is liberated during phase transformation. This heat is conducted away from the interface through the solid and liquid, resulting in the presence of thermal boundary layers near the interface. Across the interface, the density changes, say, from ρ^{ℓ} to ρ^{s}. Thus, if $\rho^{\mathrm{s}} > \rho^{\ell}$, so that the material shrinks upon solidification, a flow is induced toward the interface from "infinity."

If the liquid is not pure but contains solute, preferential rejection or incorporation of solute occurs at the interface. For example, if a single solute is present and its solubility is smaller in the (crystalline) solid than it is in the liquid, the solute will be rejected at the interface. This rejected material will be diffused away from the interface through the solid, the liquid, or both, resulting in the presence of concentration boundary layers near the interface. The thermal and concentration boundary layer structures determine, in large part, whether morphological instabilities of the interface exist and what the ultimate microstructure of the solid becomes. Many a solidification problem of interest couples the preceding purely diffusive effects with effects of thermodynamic disequilibrium, crystalline anisotropy, and convection in the melt.

On the coarsest level of understanding, freezing is of concern only as a heat or mass transfer process. Thus, one cools a glass of bourbon by inserting ice cubes that extract heat by melting. Likewise, one places salt on icy roads in Evanston to facilitate melting because salt water has a lower melting temperature than pure water.

On a finer level of understanding, freezing can create solids whose microstructures are determined by the process parameters and the intrinsic instabilities of the solid–liquid front. Figure 1.1 shows a longitudinal section of a Zn–Al alloy casting. Notice the dendritic structures that extend inward from the cold boundary and a core region in which no microstructure is visible. At later times, spontaneous nucleation in the core can cause "snowflakes" to grow in the core. The coarseness or fineness of the microstructure helps determine whether mechanical and thermal reprocessing can be accomplished without the appearance of cracks.

Under certain conditions of freezing, the moving solidification front can be susceptible to traveling-wave instabilities, giving structural patterns that can be made visible; see Figure 1.2.

When a eutectic alloy is frozen, the solid can take the form of a lamellar structure, alternate plates of two alloys spatially periodic perpendicular to the freezing direction. Under certain conditions this mode of growth is stable, giving rise to the more complex modes of growth, an example of which is shown in Figure 1.3.

Under conditions of rapid solidification, the microstructure can take on metastable states and patterns inconsistent with equilibrium thermodynamics. Figure 1.4 shows a banded structure in an Al–Cu alloy consisting of alternate layers of structured and unstructured material spatially periodic in the freezing direction. The structured layers may contain cells, dendrites, or eutectic material, whereas the alternate layers seem to have no visible microstructure.

If the solidification process occurs in a gravitational field, the thermal and solutal gradients may induce buoyancy-driven convection, which is known to affect the interfacial patterns greatly and, hence, the solidification microstructures present in the solidified material. The coupling of fluid flow in the melt with phase transformation at the interface can result in changes of microstructure scale and pattern due to alterations of frontal instabilities and the creation of new ones.

When an alloy is frozen at moderate speeds and dendritic arrays are formed, interesting dynamics occur in the dendrite–liquid mixture – the mushy zone. Here, solutal convection can be localized, creating channels parallel to the freezing direction, as shown in Figure 1.5. The channels frozen into the solid are called freckles, and their presence can significantly weaken the structure of the solid.

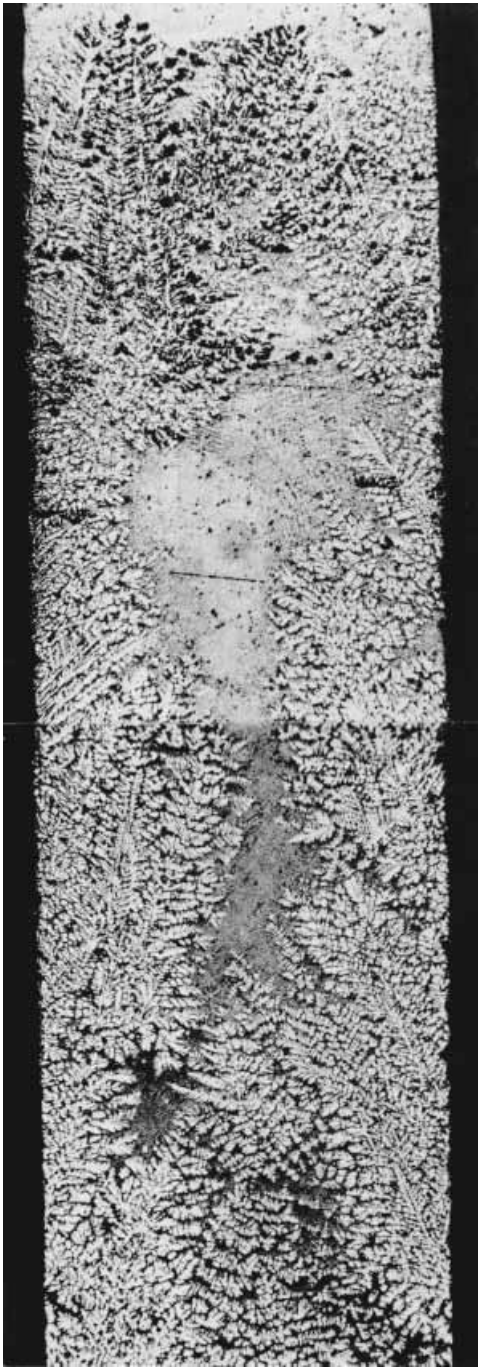

Figure 1.1. Longitudinal section of the quenched interface of the Zn–27%Al alloy. From Ayik et al. (1986).

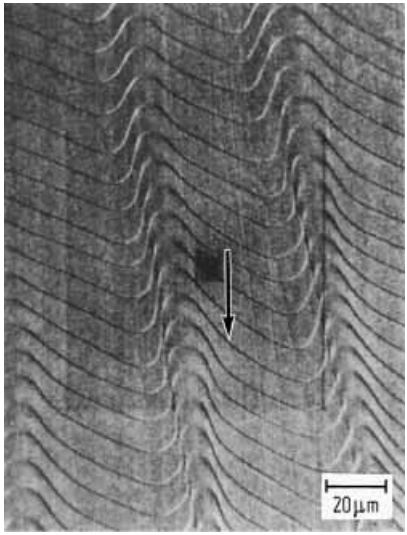

Figure 1.2. Etched longitudinal section of a Ga-doped Ge single crystal showing traveling waves on the interface. The *arrow* indicates the growth direction. From Singh, Witt, and Gatos (1974).

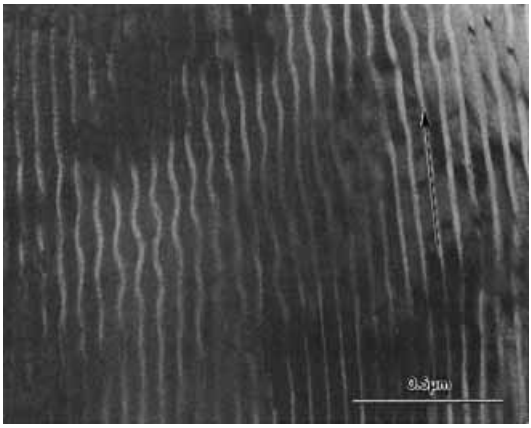

Figure 1.3. TEM micrographs of laser rapidly solidified Al–40 wt % Cu alloy oscillatory instabilities. $V = 0.03$ m/s. From Gill and Kurz (1993).

Given that the solid has crystalline structure, intrinsic symmetries in the material properties help define the continuum material. The surface energy and the kinetic coefficient on the interface as well as the bulk transport properties inherit the directional properties of the crystal, and thus anisotropies are often significant in determining the cellular or dendritic patterns that emerge. If the anisotropy is strong enough, the front can exhibit facets and corners.

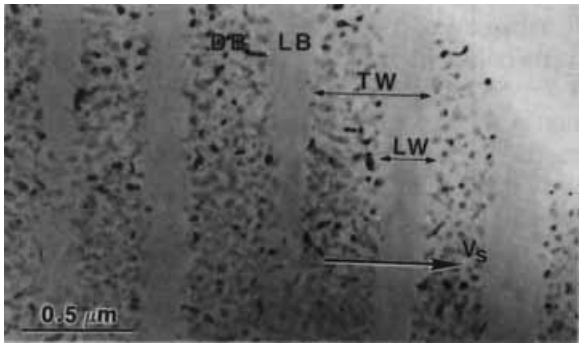

Figure 1.4. Enlarged view of the banded structure in Al–Cu 17 wt %. The dark bands have a dendritic structure, whereas the light bands are microsegregation free. DB = dark band, LB = light band, TW = total bandwidth, LW = light bandwidth, and V_s = growth rate. From Zimmermann et al. (1991).

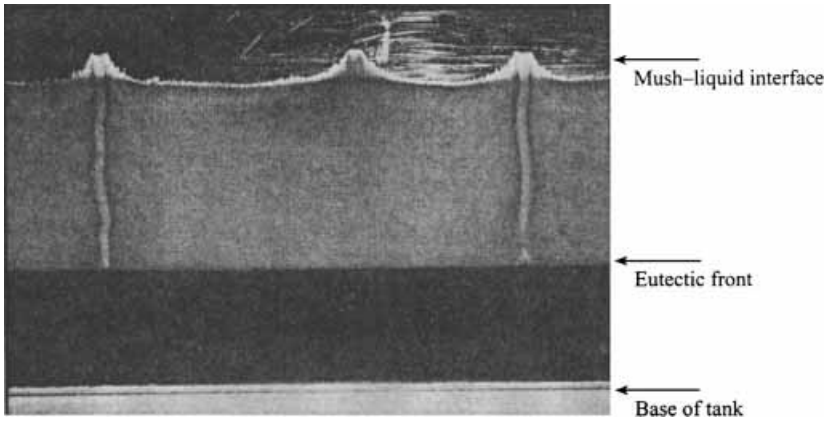

Figure 1.5. A photograph of mushy layer chimneys during an experiment with an ammonium chloride solution. In this system, pure ammonium chloride crystals are formed when the solution is cooled below its freezing temperature, leaving behind a diluted solution with a density lower than that of the bulk fluid. In the present case, the mushy layer is growing away from a fixed cold base that is at a temperature below the eutectic point, and thus both the solid–mush and mush–liquid interfaces are advancing at a decreasing rate. At the time the photograph was taken the distance between the base of the tank and the eutectic front was about 3 cm. Notice that the chimney walls and the mush–liquid interface are flat to a good first approximation. From Schulze and Worster (1998).

Finally, single crystals can be grown having, one would hope, uniform properties as long as the growth rate is very small. However, even in such cases the structure can be interrupted by defects or striations. In Figure 1.6, thermal fluctuations have created solute variations in the form of concentric rings, making the crystal inhomogeneous. If the crystal were rotated to remove azimuthal

Figure 1.6. Transverse section of a $Ba_2NaNb_5O_{15}$ crystal whose rotational striations form concentric closed loops. The striations are caused by temperature fluctuations in the melt. From Hurle (1993).

thermal variations, rotational striations could occur having the form of spirals emanating from the center of rotation.

The challenge to the scientist is to understand the sources of such inhomogeneities, quantify the phenomena at work, and learn to control the processes so as to create desired microstructures in situ on demand. Significant progress has been made in these directions, though the end point is not at hand. Clearly, this is a huge field, and inevitably an author must make subjective choices of what material to include. The view taken here is that one should delve into a "core" of the field. A grasp of the physics is developed by using examples of increasing complexity intended to create a deep physical insight applicable to more complex problems.

References

Ayik, O., Ghoreshy, M., Sahoo, M., and Smith, R. W. (1986). Solidification and foundry studies of Zn/Al alloys, *J. Crystal Growth* **79**, 594–603.

Gill, S. C., and Kurz, W. (1993). Rapidly solidified Al–Cu alloys – I. Experimental determination of the microstructure selection map, *Acta Metall. Mater*. **41**, 3563–3573.

Hurle, D. T. J. (1993). *Crystal Pulling from the Melt*, Springer-Verlag, Berlin.

Schulze, T. P., and Worster, M. G. (1998). A numerical investigation of steady convection in mushylayers during directional solidification of binary alloys, *J. Fluid Mech*. **356**, 199–220.

Singh, R., Witt, A. F., and Gatos, H. C. (1974). Oscillatory interface instability during Czochralski growth of a heavily doped germanium, *J. Electrochem. Soc*. **121**, 380–385.

Zimmermann, M., Carrard, M., Gremaud, M., and Kurz, W. (1991). Characterization of a banded structure in rapidly solidified Al–Cu alloys, *Mater. Sci. Eng.* **A134**, 1279–1282.

2

Pure substances

2.1 Planar Interfaces

2.1.1 Mathematical Model

Consider a system in thermal equilibrium so that the temperature T is uniform. Part of the system is liquid and part is solid. For the two phases to coexist, the solid–liquid interfaces must be *planar*, and the temperature must be T_{m}, the *melting temperature*; T_{m} may depend on pressure and is here taken to be constant.

The amount of heat required to change a unit *mass* of solid into liquid at $T = T_{\mathrm{m}}$ is the *latent heat* L; if ρ^{s} is the density of the solid, then the latent heat per unit volume is $L_{\mathcal{V}}$, $L_{\mathcal{V}} = \rho^{\mathrm{s}} L$. The amount of heat required to raise, without change of phase, the temperature of a unit mass of solid or liquid by 1°C is the specific heat c_p.

Consider now a system in which temperature gradients are present so that there are heat fluxes. The bulk heat balance in either phase alone can be obtained by considering a material volume $\mathcal{V}(t)$, as shown in Figure 2.1, and is given by

$$\frac{d}{dt}\int\limits_{\mathcal{V}(t)} \rho c_p T dV = -\int\limits_{\partial\mathcal{V}(t)} \mathbf{q}\cdot\mathbf{n} dS, \tag{2.1}$$

where ρ is the density, $\mathbf{q}$ is the heat flux, and $\mathbf{n}$ is the unit outward–normal vector to $\mathcal{V}$ on its (closed) boundary $\partial\mathcal{V}$.

The transport theorem for any smooth field F passing through $\mathcal{V}$ states that

$$\frac{d}{dt}\int\limits_{\mathcal{V}(t)} F dV = \int\limits_{\mathcal{V}(t)} \left[\frac{\partial F}{\partial t} + \nabla\cdot(F\mathbf{v})\right] dV, \tag{2.2}$$

where $\mathbf{v}$ is the velocity field of the material (see, e.g., Serrin 1959).

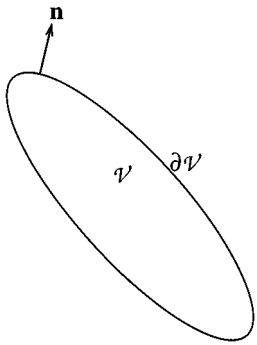

Figure 2.1. A control volume $\mathcal{V}$ entirely with a bulk phase; $\partial\mathcal{V}$ is its boundary and **n** is the unit outward normal.

If Gauss's theorem and identity (2.2) are used on relation (2.1), then

$$\int_{\mathcal{V}(t)} \left\{ \frac{\partial}{\partial t}(\rho c_p T) + \nabla \cdot (\rho c_p T \mathbf{v}) \right\} dV = - \int_{\mathcal{V}(t)} \nabla \cdot \mathbf{q} dV,$$

and since $\mathcal{V}$ is arbitrary and the integrands are supposed smooth, the point form of the bulk mass balance is obtained as

$$\frac{d}{dt}(\rho c_p T) + \rho c_p T \nabla \cdot \mathbf{v} = -\nabla \cdot \mathbf{q}, \tag{2.3}$$

where the material derivative is given by

$$\frac{d}{dt} = \frac{\partial}{\partial t} + \mathbf{v} \cdot \nabla. \tag{2.4}$$

To complete the specification of the heat balance, a constitutive law is required that relates **q** to the temperature field. It is assumed here that the Fourier law of heat conduction holds, that is

$$\mathbf{q} = -k_{\mathrm{T}} \nabla T, \tag{2.5}$$

where k_{T} is the thermal conductivity of the phase. Thus, the final form of the bulk heat balance is given by

$$\frac{d}{dt}(\rho c_p T) + \rho c_p T \nabla \cdot \mathbf{v} = \nabla \cdot k_{\mathrm{T}} \nabla T. \tag{2.6}$$

In the absence of bulk flow, $\mathbf{v} = \mathbf{0}$, and for ρ, c_p, k_{T} constant, Eq. (2.6) reduces to the standard heat-conduction equation

$$\frac{\partial T}{\partial t} = \kappa \nabla^2 T, \tag{2.7}$$

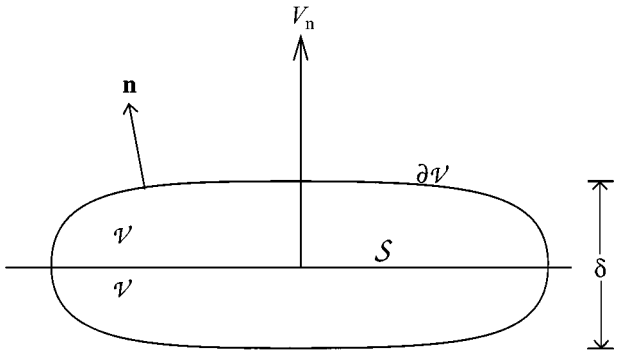

Figure 2.2. A control voume $\mathcal{V}$ spanning the interface $\mathcal{S}$ that moves at speed V_n normal to itself: $\partial\mathcal{V}$ is the boundary of $\mathcal{V}$ and $\mathbf{n}$ is the unit outward normal.

where

$$\kappa = k_T/\rho c_p$$

is the thermal diffusivity of the phase.

On a moving (planar) interface, there is a heat balance. Consider a (two-dimensional) volume of height δ spanning the interface, as shown in Figure 2.2. If V_n is the speed of the interface (normal to itself), then in a time δt and for $\delta \to 0$,

$$\rho^s L V_n \delta t = (\mathbf{q}_\ell - \mathbf{q}_s) \cdot \mathbf{n} \delta t$$

because the (smooth) heat accumulation vanishes as $\delta \to 0$. Thus, if Fourier heat conduction is applied, Eq. (2.5), the interfacial heat balance is

$$\rho^s L V_n = (k_T^s \nabla T^s - k_T^\ell \nabla T^\ell) \cdot \mathbf{n}. \tag{2.8}$$

One sees that the net heat entering the interface, the right-hand side, determines the speed V_n of the front.

In addition, the temperature is continuous across the interface and is known to be the equilibrium melting temperature T_m,

$$T^s = T^\ell = T_m. \tag{2.9}$$

2.1.2 One-Dimensional Freezing from a Cold Boundary

Consider a plane boundary at $z = 0$, which is adjacent to a liquid at initial temperature $T = T_m$, as shown in Figure 2.3. At $t = 0$, the boundary is impulsively

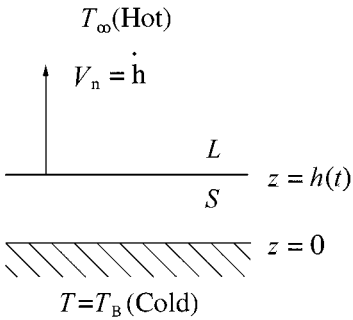

Figure 2.3. Planar solidification from a cold boundary at $z = 0$ with temperature T_B into a warmer melt at temperature T_∞. The interface between solid and liquid is at $z = h(t)$.

cooled to a temperature T_B, such that the undercooling ΔT is

$$\Delta T = T_m - T_B > 0, \tag{2.10}$$

creating a solid–liquid interface at $z = h(t)$ and it will be supposed that $\rho^s = \rho^\ell$.

Because for $t < 0$, $T = T_m$, the temperature in the liquid will not fall below T_m, hence, the temperature in the liquid is constant for all time,

$$T^\ell = T_m \qquad z > h(t). \tag{2.11a}$$

In the solid there is heat conduction

$$T^s_t = \kappa^s T^s_{zz} \qquad 0 < z < h(t). \tag{2.11b}$$

For $t > 0$

$$T^s = T_B \qquad z = 0 \tag{2.11c}$$

$$T^\ell = T^s = T_m \qquad z = h(t) \tag{2.11d}$$

$$\rho^s L\dot{a} = k^s_T T^s_z \qquad z = h(t). \tag{2.11e}$$

For $t = 0$,

$$T^s = T_m, \quad h = 0. \tag{2.11f}$$

Note that the heat flux in the liquid is zero because the temperature there is constant.

There are no natural time and space scales here, and therefore a similarity solution can be sought. Let the new independent variable be η,

$$\eta = \frac{z}{2\sqrt{\kappa^s t}}, \tag{2.12a}$$

define the nondimensional temperature by θ,

$$T^{\mathrm{s}} = T_{\mathrm{b}} + (\Delta T)\theta(\eta), \tag{2.12b}$$

and thus $\theta = 0$ at the base and $\theta = 1$ at the front. Finally, consistent with the preceding equations, the interface position is written as

$$h(t) = 2\Lambda\sqrt{\kappa^{\mathrm{s}} t}, \tag{2.12c}$$

where the value of Λ, as yet unknown, determines the speed and position of the front. Through the use of these forms, system (2.11a) becomes

$$\theta'' + 2\eta\theta' = 0 \qquad 0 < \eta < \Lambda \tag{2.13a}$$

$$\theta = 0 \qquad \eta = 0 \tag{2.13b}$$

$$\theta = 1 \qquad \eta = \Lambda \tag{2.13c}$$

$$\theta' = 2S\Lambda \qquad \eta = \Lambda \tag{2.13d}$$

where the Stefan number S is

$$S = \frac{L}{c_p^{\mathrm{s}} \Delta T}. \tag{2.14}$$

Notice that the initial conditions (2.11f) applied at $t = 0$ corresponds to $\eta \to \infty$ and that the temperature is constant in (h, ∞). Thus, the thermal condition can be applied at $\eta = \Lambda$, as shown in Eq. (2.13c). One integral of Eq. (2.13a) gives

$$\theta' = Ae^{-\eta^2}, \tag{2.15a}$$

where the integration constant A satisfies

$$2S\Lambda = Ae^{-\Lambda^2}. \tag{2.15b}$$

A second integral that satisfies Eqs. (2.13b,c) is

$$\theta = \frac{\displaystyle\int_0^{\eta} e^{-s^2} ds}{\displaystyle\int_0^{\Lambda} e^{-s^2} ds} = \frac{\mathrm{erf}\,(\eta)}{\mathrm{erf}\,(\Lambda)}, \tag{2.15c}$$

where the error function is defined by

$$\mathrm{erf}\,(z) \equiv \frac{2}{\sqrt{\pi}} \int_0^{z} e^{-s^2} ds. \tag{2.16}$$

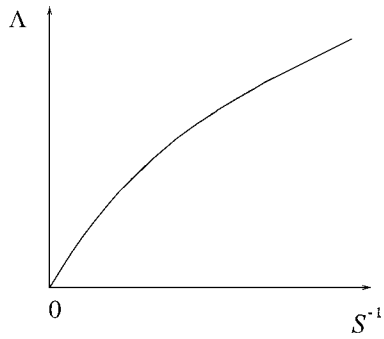

Figure 2.4. A sketch of Eq. (2.17) for the interface speed Λ versus the undercooling S^{-1}. Solutions exist for all S^{-1}.

When form (2.15c) is substituted into the flux condition (2.13d), one finds that

$$\sqrt{\pi}\,\Lambda e^{\Lambda^2}\mathrm{erf}\,(\Lambda) = S^{-1}, \tag{2.17}$$

which gives $\Lambda = \Lambda(S)$, the speed of the front as a function of the undercooling, as shown in Figure 2.4.

Notes

1. Solutions exist for all values of the nondimensional undercooling S^{-1}.
2. Notice that $h \sim t^{1/2}$, and hence $\dot{h} \sim t^{-1/2}$. The solution fails at $t = 0$, where the front speed is infinite (owing to the assumption of impulsive heating) and decreases with time.
3. The temperature gradient G_{T} at the interface is

$$\begin{aligned} G_{\mathrm{T}} = T_z^{\mathrm{s}}\,|_{z=h} &= \frac{\Delta T}{2\sqrt{\kappa^{\mathrm{s}} t}}\theta'(\eta)\,|_{\eta=\Lambda} \\ &= \frac{\Delta T}{\sqrt{\kappa^{\mathrm{s}} t}}\Lambda S > 0, \end{aligned} \tag{2.18}$$

   and thus the heat flows downward through the solid. Consequently, the front speed depends on κ^{s}, and not κ^{ℓ}. As will be seen, $G_{\mathrm{T}} > 0$ indicates that the front is stable to disturbances periodic along the front.
4. If, initially, one sets the temperature of the liquid at $T^{\ell} = T_{\infty} > T_{\mathrm{m}}$, then there would also be heat flow in the liquid and the profiles would look as shown in Figure 2.5; the front speed would then depend on both diffusivities. In both cases T is continuous at $z = h(t)$, but the gradient T_z is not.
5. The similarity solution posed is a "preferred" solution in the sense that, under rather weak conditions, all solutions of the initial-value problem (2.11) approach the similarity solution as $t \to \infty$.
6. When S^{-1} is small, ΔT is small or L is large. Figure 2.4 or Eq. (2.17) shows that Λ is small so that freezing takes place very slowly. It is useful to analyze the limit of small ΔT separately.

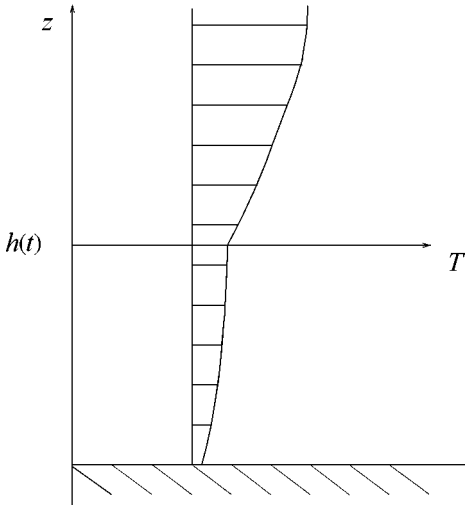

Figure 2.5. A sketch of the temperature profiles in the solid and liquid for the two-phase conduction problem.

2.1.3 One-Dimensional Freezing from a Cold Boundary: Small Undercooling

When $S^{-1} \equiv \epsilon \ll 1$, then the growth rate is small. Scale the original system Eqs. (2.11) as follows:

$$\zeta = z/\ell, \quad \tau = t/t_o \tag{2.19a}$$

$$A(\tau) = h(t)/\ell, \quad T^{\mathrm{s}}(z,t) = T_{\mathrm{B}} + (\Delta T)\theta(\zeta,\tau), \tag{2.19b}$$

where ℓ and t_o are scales undefined for the moment. From the previous solution it is seen that heat conduction in the solid is important; therefore let $t_o = \ell^2/\kappa^{\mathrm{s}}$. System (2.11) then becomes

$$\theta_\tau = \theta_{\zeta\zeta} \qquad 0 < \zeta < A(\tau) \tag{2.20a}$$

$$\theta = 0 \qquad \zeta = 0 \tag{2.20b}$$

$$\theta = 1 \qquad \zeta = A(\tau) \tag{2.20c}$$

$$A_\tau = \epsilon\theta_\zeta \qquad \zeta = A(\tau) \tag{2.20d}$$

$$\left.\begin{aligned} A &= A_0 \\ \theta(\zeta,0) &= \theta_0(0) \end{aligned}\right\}, \quad \tau = 0. \tag{2.20e}$$

In the preceding, the problem has been generalized to allow nonzero initial temperature distributions $\theta_0(\zeta)$ and initial-front positions A_0.

If $\partial/\partial\tau = O(1)$ and $\epsilon \to 0$, the resulting system remains second order in time and hence is capable of satisfying both initial conditions. However, at first approximation $A_\tau \sim 0$, and thus from time zero to $\tau = O(1)$ the interface is stationary at its initial position and solidification does not occur. In this time interval one then has a standard heat-conduction problem for θ on a fixed domain, $0 < \zeta < A$. This represents the *inner solution in time*. The *outer solution in time*, valid for long periods, requires a rescaling of time

$$\hat{\tau} = \epsilon\tau, \tag{2.21}$$

which represents a time scale based on latent heat and undercooling, namely $\rho^{\mathrm{s}} L\ell^2/k_{\mathrm{T}}\Delta T$, and so describes the solidification process. In this case, system (2.11) becomes

$$\epsilon\theta_{\hat{t}} = \theta_{\zeta\zeta} \qquad 0 < \zeta < A(\hat{\tau}) \tag{2.22a}$$

$$\theta = 0 \qquad \zeta = 0 \tag{2.22b}$$

$$\theta = 1 \qquad \zeta = A(\hat{\tau}) \tag{2.22c}$$

$$A_{\hat{t}} = \theta_\zeta \qquad \zeta = A(\hat{\tau}) \tag{2.22d}$$

$$A = A_0,\ \theta = \theta_0 \qquad \hat{\tau} = 0. \tag{2.22e}$$

The limit $\partial/\partial\hat{\tau} = O(1)$ and $\epsilon \to 0$ is a singular perturbation; it is seen that at first approximation the temperature is quasi-steady,

$$\theta_{\zeta\zeta} = 0. \tag{2.23}$$

The solution that satisfies Eqs. (2.22b,c) is

$$\theta = \zeta/A. \tag{2.24}$$

Now the flux condition (2.22d) gives

$$AA_{\hat{t}} = 1, \tag{2.25}$$

which is a nonlinear evolution equation for A (Young 1994). Thus, with the first of condition (2.22e),

$$A^2(\hat{\tau}) - A_0^2 = 2\hat{\tau}. \tag{2.26}$$

In dimensional terms,

$$h^2 - h_0^2 = 2\epsilon\kappa^{\mathrm{s}} t = \frac{2k_{\mathrm{T}}^{\mathrm{s}}(\Delta T)t}{\rho^{\mathrm{s}} L}. \tag{2.27}$$

The inner and outer solutions automatically match asymptotically.

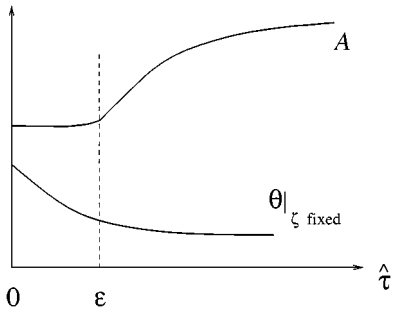

Figure 2.6. Sketches of the temperature and interface position as functions for the outer time $\hat{t}$ for small ϵ.

Solution (2.27) coincides with the similarity solution for $S \to \infty$ and $h_0 = 0$ where $h = 2\Lambda\sqrt{\kappa^s t}$ and $\Lambda \sim (2S)^{-1/2}$.

Note: The length scale ℓ was never defined, and because the original problem has no intrinsic length scale, ℓ cancels from the results, as seen in Eq. (2.27).

The solutions can be sketched symbolically, as shown in Figure 2.6. For $\hat{\tau} \sim \epsilon$, $\tau \sim 1$, A is constant, and θ develops. For $\hat{\tau} \sim 1$, θ is quasi-steady, and its time evolution is determined by that of A, as shown.

2.1.4 One-Dimensional Freezing into an Undercooled Melt

Consider the semi-infinite body of fluid shown in Figure 2.7 that is cooled below T_m to T_∞, $\Delta T = T_m - T_\infty$.

At $t = 0$, a plate is inserted at $z = 0$ at temperature T_m. For $\rho^s = \rho^\ell$, one wishes to determine how the system evolves. The temperature profile at a fixed time is shown in Figure 2.8; in the solid, $T = T_m$ always, and thus heat conduction is absent there.

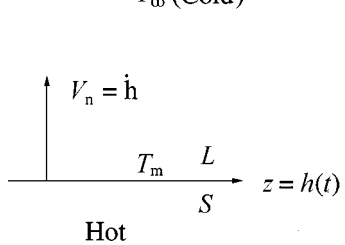

Figure 2.7. Planar solidification into an undercooled melt, where the interface has position $z = h(t)$.

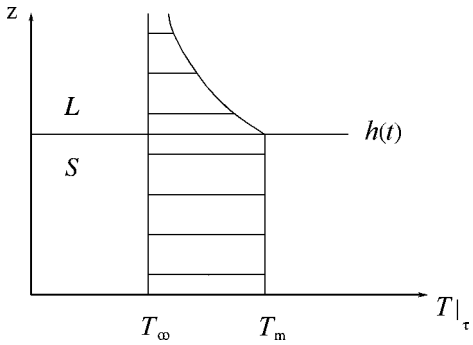

Figure 2.8. A sketch of the temperature profiles for planar solidification into an undercooled melt.

The governing system is as follows:
In solid, $z < h(t)$,

$$T^{\mathrm{s}} = T_{\mathrm{m}} \tag{2.28a}$$

In liquid, $z > h(t)$,

$$T_t^{\ell} = \kappa^{\ell} T_{zz}^{\ell} \tag{2.28b}$$

As $z \to \infty$,

$$T^{\ell} \to T_{\infty} \tag{2.28c}$$

On $z = h(t)$

$$T^{\ell} = T^{\mathrm{s}} = T_{\mathrm{m}}. \tag{2.28d}$$

$$\rho^{\mathrm{s}} L\dot{h} = -k_{\mathrm{T}}^{\ell} T_z^{\ell}. \tag{2.28e}$$

Again, because there are no natural spatial and time scales in the problem, a similarity solution can be sought. Let the new independent variable be

$$\eta = \frac{z}{2\sqrt{\kappa^{\ell} t}}, \tag{2.29a}$$

and let the scaled temperature be θ,

$$T^{\ell} = T_{\infty} + (\Delta T)\theta(\eta). \tag{2.29b}$$

For consistency, let

$$h = 2\Lambda\sqrt{\kappa^{\ell} t}, \tag{2.29c}$$

where the speed coefficient Λ is to be determined.

The solution for the temperature is

$$\theta(\eta) = \frac{\operatorname{erfc}(\eta)}{\operatorname{erfc}(\Lambda)}, \tag{2.30}$$

where the complementary error function is defined by

$$\operatorname{erfc}(z) = \frac{2}{\sqrt{\pi}} \int_z^\infty e^{-s^2} ds. \tag{2.31}$$

The flux condition (2.28e) then gives the characteristic equation

$$\sqrt{\pi}\,\Lambda e^{\Lambda^2} \operatorname{erfc}(\Lambda) = S^{-1}. \tag{2.32}$$

Note: The temperature gradient G_{T} in the liquid at the interface

$$G_{\mathrm{T}} = T_z[h(t), t] < 0$$

always, and thus the heat flows through the liquid. Consequently, the front speed depends on κ^ℓ and not κ^{s}. As will be seen, $G_{\mathrm{T}} < 0$ indicates that the front is unstable to disturbances periodic along the front.

If one plots Eq. (2.32), Figure 2.9 is obtained. The curve approaches $S^{-1} = 1$, which is called *unit undercooling*. There exist *no* solutions for $S^{-1} \geq 1$. Note that as $S^{-1} \to 1^-$, $\Lambda \to \infty$, and thus the front speed approaches infinity. This suggests the breakdown of the validity of the thermodynamic equilibrium assumption appropriate to relatively small front speeds.

Solidification is a surface reaction whose rate depends upon the degree of undercooling that drives it. The argument of Worster (private communication 1993) will be followed. At $T^{\mathrm{I}} = T_{\mathrm{m}}$ a solid–liquid interface is in a dynamic equilibrium with molecules attaching and detaching continually and at equal rates. When $T^{\mathrm{I}} < T_{\mathrm{m}}$, molecules become more strongly bound to the interface

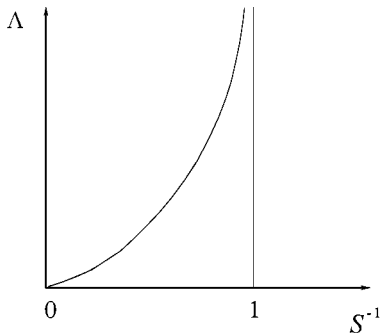

Figure 2.9. A sketch of Eq. (2.32) for the interface speed Λ versus the undercooling S^{-1}. Solutions exist only for $S^{-1} < 1$.

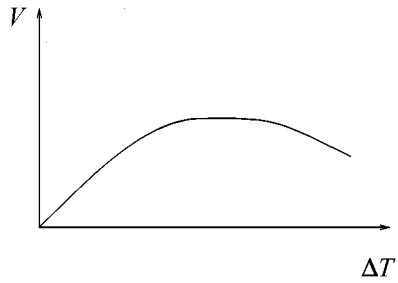

Figure 2.10. A sketch of the kinetic undercooling versus the speeds.

and thus the number detaching per unit time decreases and the interface advances at speed V_n; V_n increases with $T_m - T^I$. However, as T^I decreases further, the molecules in the liquid become sluggish and the rate of attachment decreases. Hence, the figure presumably looks like Figure 2.10. This relation may in fact not be a simple function of V directly, but a more complicated functional (Bates, Fife, Gardner, and Jones 1997). Here the model of Figure 2.10 will be used.

For ΔT small, the graph depends on the mode of attachment (e.g., by adding molecular planes, screw dislocations, or random attachments). However, for substances (e.g., metals) having low latent heats, V_n can be approximated as a linear function of ΔT,

$$V_n = \mu(T_m - T^I), \tag{2.33}$$

where the positive constant μ is called the *kinetic coefficient*. Equation (2.33) can be rewritten as

$$T^I = T_m - \mu^{-1} V_n \tag{2.34}$$

and represents the effect of *kinetic undercooling*.

Equation (2.34) determines the interfacial temperature for each front speed V_n. The presence of kinetic undercooling, $\mu^{-1} \neq 0$, lowers the interfacial temperature below that in equilibrium.

As will be seen in a moment, replacing Eqn. (2.28d) by (2.34), makes solutions possible for all ΔT.

2.1.5 One-Dimensional Freezing into an Undercooled Melt: Effect of Kinetic Undercooling

The generalized governing system now takes the form

In solid, $z < h(t)$,

$$T^s = T^I \tag{2.35a}$$

In liquid, $z > h(t)$

$$T_t^\ell = \kappa^\ell T_{zz}^\ell \tag{2.35b}$$

As $z \to \infty$

$$T^\ell \to T_\infty \tag{2.35c}$$

On $z = h(t)$,

$$T^\ell = T^{\mathrm{I}}, \tag{2.35d}$$

$$\rho^{\mathrm{s}} L\dot{h} = -k^\ell T_z^\ell, \tag{2.35e}$$

$$\dot{h} = \mu(T_{\mathrm{m}} - T^{\mathrm{I}}). \tag{2.35f}$$

Notice here that T^{I} is now unknown and must be determined as part of the solution.

An important difference between the equilibrium and nonequilibrium formulations is seen by dimensional analysis. Previously, the scales of length ℓ and time t_o were arbitrary, and a relation between them associated with heat conduction, $t_o = \ell^2/\kappa^\ell$, was used; however, ℓ was still arbitrary. Now, however, ℓ is determined by the kinetic undercooling, namely

$$\ell\left(\frac{\kappa^\ell}{\ell^2}\right) = \mu\Delta T,$$

and thus

$$\ell = \frac{\kappa^\ell}{\mu\Delta T}; \tag{2.36a}$$

hence, using $t_o = \ell^2/\kappa^\ell$, we obtain

$$t_o = \frac{\kappa^\ell}{\mu^2(\Delta T)^2}. \tag{2.36b}$$

Write again

$$T^\ell = T_\infty + (\Delta T)\theta, \tag{2.37}$$

and the scaled system becomes

$$\theta_t = \theta_{zz} \qquad z > A(t) \tag{2.38a}$$

$$\theta \to 0 \qquad z \to \infty \tag{2.38b}$$

$$\left.\begin{array}{c} \theta = \theta^{\mathrm{I}} \\ S\dot{A} = -\theta_z \\ \dot{A} = 1 - \theta^{\mathrm{I}} \end{array}\right\}, \quad z = A(t) \tag{2.38c}$$

The kinetic condition suggests seeking a solution with θ^{I} constant; hence, $\dot{A}(t) = V$. Let us seek a traveling-wave solution

$$\theta = \theta(\zeta), \tag{2.39a}$$

where

$$\zeta = z - Vt, \tag{2.39b}$$

and so the interface lies at $\zeta = 0$. Here V is a constant and ζ is measured in a moving frame of reference. The diffusion equation (2.38a) then becomes

$$-V\theta' = \theta'', \tag{2.40}$$

where a prime denotes $d/d\zeta$.

The solution of Eq. (2.40), subject to conditions (2.38b) and the first of (2.38c), is

$$\theta = \theta^{\mathrm{I}} e^{-V\zeta}. \tag{2.41}$$

The Stefan and kinetic conditions, the second and third of Eqs. (2.38c) then give

$$\theta^{\mathrm{I}} = S \tag{2.42}$$

and

$$V = 1 - S, \quad S < 1. \tag{2.43}$$

Thus, for all $S < 1$,

$$\theta = Se^{-(1-S)(z-Vt)}, \tag{2.44}$$

and solutions for $S^{-1} > 1$ have been found (Glicksman and Schaefer 1967).

Note: Again, $G_{\mathrm{T}} < 0$.

When there is unit undercooling, $S = 1$, yet a different solution exists (Umantsev 1985) with $h(t) \sim t^{2/3}$. With kinetic undercooling present, there are solutions for all S:

$$\left.\begin{array}{ll} S^{-1} < 1, & h \sim t^{\frac{1}{2}} \\ S^{-1} = 1, & h \sim t^{\frac{2}{3}} \\ S^{-1} > 1, & h \sim t \end{array}\right\}. \tag{2.45}$$

2.2 Curved Interfaces

2.2.1 Boundary Conditions

Consider a two-dimensional solid "drop" on a substrate, as shown in Figure 2.11; no phase transformation is present. Thermodynamic equilibrium implies that the Helmholtz free energy E of the system, the sum of the surface energies, must be at a minimum for an equilibrium state to exist. Note that other energies, such as the elastic energy of "drop" and substrate, are ignored here, as is usual. The analysis follows Mullins (1963).

Let the system be uniform in the direction normal to the page and let w be a unit of length in that direction. The Helmholtz free energy is then

$$E = w\left\{\int_{\ell_1}^{\ell_2} \gamma\left(1+h_x^2\right)^{1/2} dx + \gamma_1(\ell_2-\ell_1) + \gamma_2[\ell-(\ell_2-\ell_1)]\right\}, \quad (2.46a)$$

where $z = h(x)$ is the height of the interface, γ is the energy per unit area on the drop–liquid interface, and γ_1 and γ_2 are the corresponding surface energies per unit area on the solid–substrate and liquid–substrate interfaces, respectively; all of these are taken to be constants, ℓ is a fixed length, always larger than drop width, which is introduced to keep the energies finite; $x = \ell_1$and ℓ_2 are the endpoints of the drop, and θ, measured within the drop, is called the contact angle. Consider variations in h, ℓ_1, and ℓ_2 such that the volume $\mathcal{V}$ of the drop is preserved, where

$$\mathcal{V} = w\int_{\ell_1}^{\ell_2} h dx. \quad (2.46b)$$

For a discussion of the variational calculus needed for this section, see Courant and Hilbert (1953), Chap. 4.

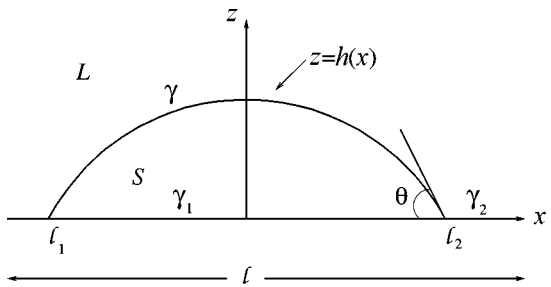

Figure 2.11. A solid, two-dimensional drop on a substrate; $z = h(x)$ is the drop shape, $x = \ell_1$ and ℓ_2 are the locations of the contact lines, ℓ indicates an expanse larger than the drop, and θ is the contact angle.

The constrained problem defined above can be written as an unconstrained variational problem by introducing the Lagrange multiplier λ and writing

$$E' = E + \lambda w \int_{\ell_1}^{\ell_2} h dx$$
$$= w \left\{ \int_{\ell_1}^{\ell_2} \left[\gamma \left(1 + h_x^2\right)^{1/2} + \lambda h \right] dx + \gamma_1(\ell_2 - \ell_1) + \gamma_2 \left[\ell - (\ell_2 - \ell_1)\right] \right\}. \tag{2.47}$$

In order for E' to be minimum, it is necessary for the first variation, $\delta E'$, to be zero,

$$w^{-1}\delta E' = \int_{\ell_1}^{\ell_2} \left\{ \frac{\gamma h_x \delta(h_x)}{\left(1 + h_x^2\right)^{1/2}} + \lambda \delta h \right\} dx$$
$$+ \left\{ \gamma \left[\left(1 + h_x^2\right)^{1/2} \right] + \lambda h \Big|_{\ell_2} + \gamma_1 - \gamma_2 \right\} \delta \ell_2$$
$$+ \left\{ -\gamma \left[\left(1 + h_x^2\right)^{1/2} \right] - \lambda h \Big|_{\ell_1} - \gamma_1 + \gamma_2 \right\} \delta \ell_1 = 0 \tag{2.48}$$

Formally, one writes that

$$\delta(h_x) = (\delta h)_x \tag{2.49}$$

and uses integration by parts to obtain

$$\int_{\ell_1}^{\ell} \frac{h_x \delta h_x}{\left(1 + h_x^2\right)^{1/2}} dx = -\int_{\ell_1}^{\ell_2} \left\{ \frac{h_x}{\left(1 + h_x^2\right)^{1/2}} \right\}_x \delta h \, dx + \frac{h_x \delta h}{\left(1 + h_x^2\right)^{1/2}} \Bigg|_{\ell_1}^{\ell_2}. \tag{2.50}$$

Figure 2.12 shows a neighborhood of the right-hand contact line at $x = \ell_2$. One can then write that

$$\delta h \,\big|_{\ell_2} = -h_x \delta \ell \big|_{\ell_2}, \tag{2.51a}$$

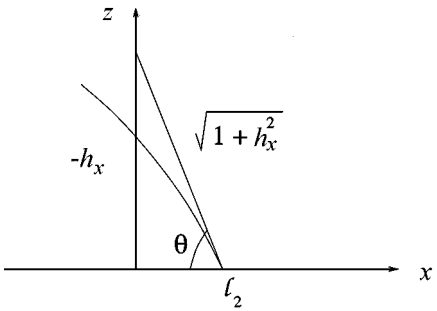

Figure 2.12. A close-up of the local geometry of the contact-line region near $x = \ell_2$ of Figure 2.11.

and similarly at the other contact line

$$\delta h\,\big|_{\ell_1} = -h_x \delta\ell\big|_{\ell_1} \tag{2.51b}$$

Thus,

$$\left.\frac{h_x \delta h}{\left(1+h_x^2\right)^{1/2}}\right|_{\ell_1}^{\ell_2} = -\left.\frac{h_x^2 \delta\ell}{\left(1+h_x^2\right)^{1/2}}\right|_{\ell_1}^{\ell_2}. \tag{2.52}$$

Finally,

$$\begin{aligned} w^{-1}\delta E' = \int_{\ell_1}^{\ell_2} & \left\{ -\gamma \left[\frac{h_x}{\left(1+h_x^2\right)^{1/2}} \right]_x + \lambda \right\} \delta h \, dx \\ & + \left\{ \left. \frac{\gamma}{\left(1+h_x^2\right)^{1/2}} \right|_{\ell_2} + \lambda h + \gamma_1 - \gamma_2 \right\} \delta\ell_2 \\ & - \left\{ \left. \frac{\gamma}{\left(1+h_x^2\right)^{1/2}} \right|_{\ell_1} + \lambda h + \gamma_1 - \gamma_2 \right\} \delta\ell_1 = 0, \end{aligned} \tag{2.53}$$

where the boundary terms have been combined.

Consider first variations in which the endpoints are fixed, that is, $\delta\ell_1 = \delta\ell_2 = 0$. Given that the integrand of Eq. (2.53) is smooth and δh is otherwise arbitrary, that integrand must vanish. This gives the Euler–Lagrange equation

$$-\gamma \left[\frac{h_x}{\left(1+h_x^2\right)^{1/2}} \right]_x + \lambda = 0$$

or

$$2H\gamma = \lambda \tag{2.54}$$

Here, for a one-dimensional interface the mean curvature H is defined by

$$2H = \frac{h_{xx}}{\left(1+h_x^2\right)^{3/2}}. \tag{2.55}$$

The interfacial shape h has constant curvature, and thus in two dimensions is an arc of a circle. By this definition a solid finger extending into the liquid has $H < 0$. The Lagrange multiplier is a constant that cannot be determined by variational calculus but requires some additional physical statement (Hills and Roberts 1993).

Let the Gibbs free energy Φ of the system depend on the pressure p and the temperature T. Let Φ on the solid side of the interface be equal to that on the

liquid side. Expand this equation about $p = p^{\ell}$, the pressure on the liquid side, let $T = T_{\mathrm{m}}$ and identify $\partial\Phi/\partial p$ by $1/p^{\mathrm{s}}$, and let $\partial\Phi/\partial T = -s$, the entropy, and $\Delta s = L_{\nu}/T_{\mathrm{m}}$,; then one can write

$$\lambda = L_{\nu}\Delta T/T_{\mathrm{m}}, \tag{2.56a}$$

where

$$\Delta T = T^{\mathrm{I}} - T_{\mathrm{m}}. \tag{2.56b}$$

Here T^{I} is the drop–liquid interface temperature and T_{m} is the equilibrium melting temperature of the material in the drop.

The results above can be obtained by using the total grand potential (Gibbs 1948, p. 229; Wettlaufer and Worster 1995), and this approach has the advantage of easy generalization to multicomponent systems.

Equation (2.54) is the Laplace relation for the interface, and the following is the Gibbs–Thomson relation giving *capillary undercooling*:

$$T^{\mathrm{I}} = T_{\mathrm{m}}\left[1 + 2H\frac{\gamma}{L_{\nu}}\right] \tag{2.57}$$

If H is replaced by its generalization to a two-dimensional surface, then Eq. (2.57) holds for three-dimensional systems. See Chapter 5 for generalizations to systems where γ depends on the orientation of the surface.

Consider next variations in which the endpoints may move. Because Eq. (2.54) holds already, one has at each endpoint $x = \ell_i$, $i = 1, 2$, that

$$\frac{\gamma}{\left(1 + h_x^2\right)^{1/2}} + \gamma_1 - \gamma_2 = 0, \tag{2.58}$$

because h is zero at the endpoints. If Figure 2.12 is used to evaluate this, $\left(1 + h_x^2\right)^{-1/2} = \cos\theta$, and thus the Young–Laplace relation emerges,

$$\gamma\cos\theta = \gamma_2 - \gamma_1. \tag{2.59}$$

At equilibrium at each contact line the contact angle θ adjusts itself to give this surface–energy balance. See Chapter 5 for generalizations to systems where γ depends on the orientation of the surface.

On a moving interface, there is a heat balance, applied to the domain shown in Figure 2.13. Call V_{n} the speed of the interface normal to itself and s the arc length. In Figure 2.13 as $\delta \to 0$ in a time δt,

$$\rho^{\mathrm{s}} L V_{\mathrm{n}} A\delta t - \gamma A\,|_{s+\delta s} + \gamma A|_s = (\mathbf{q}_{\ell} - \mathbf{q}_s)\cdot\mathbf{n}A\delta t$$

or

$$\rho^{\mathrm{s}} L V_{\mathrm{n}} - \frac{1}{A}\frac{\partial}{\partial t}(\gamma A) = k_{\mathrm{T}}^{s} T_n^{s} - k_{\mathrm{T}}^{\ell} T_n^{\ell}. \tag{2.60}$$

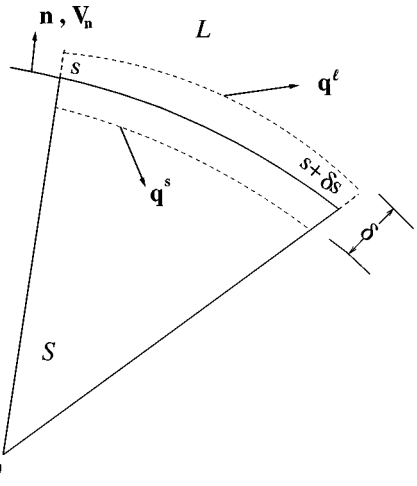

Figure 2.13. A sketch of a sector of interface from s to $s + \Delta s$ and a control volume spanning it.

One can obtain an identity from differential geometry (e.g., see Aris 1989),

$$\frac{1}{A}\frac{\partial A}{\partial t} = -2HV_{\mathrm{n}}, \tag{2.61}$$

where $\partial A/\partial t$ represents the stretching of the area A. Hence,

$$(\rho^{\mathrm{s}}L + 2H\gamma)V_{\mathrm{n}} = (k_{\mathrm{T}}^{s}\nabla T^{\mathrm{s}} - k_{\mathrm{T}}^{\ell}\nabla T^{\ell}) \cdot \mathbf{n}. \tag{2.62}$$

The usual form of this heat balance ignores the second term on the left-hand side, which was first derived by Wollkind (1979). It represents the energy expended by interfacial stretching. For a solid finger extending into the liquid $H < 0$, and thus a portion of the heat liberated by phase transformation goes into the creation of interface. For a given difference in heat fluxes, L is effectively decreased, and so V_{n} is increased.

In sum, the required conditions on a curved interface are as follows:

There is continuity of temperature

$$T^{\mathrm{I}} = T^{\mathrm{s}} = T^{\ell} \tag{2.63a}$$

and the generalized Gibbs–Thomson equation

$$T^{\mathrm{I}} = T_{\mathrm{m}}\left(1 + 2H\frac{\gamma}{L_{\nu}}\right) - \mu^{-1}V_{\mathrm{n}} \tag{2.63b}$$

where we have included the kinetic undercooling discussed earlier with V replaced by V_{n} for a curved front. Thus, the interface temperature is reduced